

Galaxy Clusters and Gamma-Ray Lines: Probing Gravitino Dark Matter with the Fermi LAT

Xiaoyuan Huang

National Astronomical Observatories, Chinese Academy of Sciences, Beijing, 100012, China

Gilles Vertongen

Institut d'Astrophysique de Paris, UMR-7095 du CNRS, 98 bis bd Arago, 75014 Paris, France

Christoph Weniger

Max-Planck-Institut für Physik, Föhringer Ring 6, 80805 München, Germany

If dark matter particles are not perfectly stable, their decay products might be seen in the cosmic-ray fluxes. A natural candidate for decaying dark matter is the gravitino in R -parity violating scenarios. In the relevant GeV-TeV energy range, the Fermi Large Area Telescope (LAT) is now measuring cosmic gamma-ray fluxes with an unprecedented precision. We use the Fermi LAT gamma-ray data to search for signatures from gravitino dark matter particles, concentrating on gamma-ray lines and galaxy cluster observations. Implications of our results for the decay length of the next-to-lightest superparticle, which could be seen at the LHC in the near future, are discussed.

I. INTRODUCTION

A theoretically well motivated example for *decaying dark matter* is the gravitino $\psi_{3/2}$, which appears in locally supersymmetric extensions of the Standard Model. In scenarios where R -parity is mildly violated and the gravitino is the lightest superparticle (LSP), thermal leptogenesis, gravitino dark matter and primordial nucleosynthesis are naturally consistent [1]. Within this framework, the gravitino would decay with cosmological lifetimes [2], making its decay products potentially observable in the cosmic-ray fluxes [3–7]. For gravitino masses $m_{3/2} \lesssim 200$ GeV, the most prominent feature in the decay spectrum is an intense gamma-ray line, produced by two-body decay into neutrinos and photons, $\psi_{3/2} \rightarrow \gamma\nu$ [4]; this line can be searched for in the gamma-ray fluxes observed at high latitudes. For larger gravitino masses $m_{3/2} \gtrsim 200$ GeV, the branching ratio into gamma-ray lines is suppressed, and instead the decay modes $\psi_{3/2} \rightarrow W^\pm \ell^\mp$ and $\psi_{3/2} \rightarrow Z^0\nu$ produce a gamma-ray flux with a broad continuous energy spectrum; this flux could potentially show up in observations of galaxy clusters or the extragalactic gamma-ray background (see *e.g.* Ref. [3, 8, 9]).

Here, we briefly summarize our searches for gamma-ray signals from gravitino dark matter in the data of the Fermi Large Area Telescope (LAT) [10]. Firstly [11], we extend the gamma-ray line analysis presented in Ref. [12] to a larger energy range of 1–300 GeV, searching for significant line signals that might come from dark matter decay (or annihilation) in the Galactic dark matter halo. Secondly [13], we analyze the gamma-ray flux from eight galaxy clusters, targets which are more sensitive to continuous spectra. Extending previous analysis [14, 15], we treat the decaying dark matter signal as extended source and analyze the different target clusters individually

as well as in a combined likelihood approach. We present constraints on the dark matter lifetime as well as on the annihilation cross section. We then apply our findings to the scenario of decaying gravitino dark matter and comment on implications for the possible observation of long-lived superparticles at the LHC.

The remaining sections are organized as follows: In the second section, we introduce briefly the gravitino dark matter scenario, in section three we summarize our gamma-ray line and galaxy cluster analysis, and in the fourth section we present the resulting limits on the gravitino lifetime and decay width of the next-to-lightest superparticle (NLSP).

II. GRAVITINO DARK MATTER

Among the different scenarios that were proposed to reconcile thermal leptogenesis and gravitino dark matter with the standard BBN scenario [16–19], a mild violation of R -parity that induces a rapid decay of the NLSP before the onset of the BBN is maybe the most interesting from the perspective of indirect dark matter searches [1]. If R -parity is violated, the gravitino dark matter particle becomes unstable and subject to decay, which opens the possibility to look for its decay products in the cosmic-ray fluxes.

Here, we consider the supersymmetric standard model with explicit bilinear R -parity violation as described in Ref. [20]. Trading the mass mixing parameters for R -parity breaking Yukawa couplings as proposed in Ref. [20], the gravitino decay is a function of a single dimensionless parameter ζ , which also enters the decay width of the NLSP. As boundary conditions for the supersymmetry breaking parameters of the MSSM at the grand unification (GUT) scale, we consider equal scalar and gaugino masses $m_0 = m_{1/2}$, a zero trilinear scalar coupling $a_0 = 0$, and $\tan\beta = 10$.

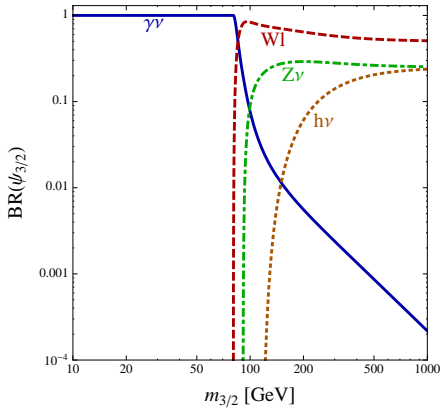


FIG. 1: Two-body decay branching ratios of the gravitino, from Ref. [13].

In this case, the bino-like neutralino $\tilde{\chi}_1^0$ is the NLSP; the universal gaugino mass $m_{1/2}$ remains as the only independent variable, and the gaugino masses $M_{1,2,3}$ satisfy the following relations at the electroweak scale: $M_3/M_1 \simeq 5.9$ and $M_2/M_1 \simeq 1.9$. Electroweak precision tests (EWPT) [20–22], as well as the possible overproduction of gravitinos in presence of the high reheating temperatures required by standard thermal leptogenesis [23], yield further bounds on the gravitino mass like $m_{3/2} \gtrsim 30$ GeV, and on the NLSP neutralino mass like $100 \text{ GeV} \lesssim m_{\tilde{\chi}_1^0} \lesssim 690 \text{ GeV}$ (for details see Ref. [11]).

The gravitino inverse decay rate into photon/neutrino pairs is given by [2, 20]

$$\Gamma_{\psi_{3/2} \rightarrow \gamma\nu}^{-1} \simeq \frac{32\sqrt{2} G_F M_P^2}{\alpha\zeta^2} \frac{M_1^2 M_2^2}{m_{3/2}^3 (M_2 - M_1)^2}, \quad (1)$$

where α is the electromagnetic fine structure constant, $M_P = 2.4 \times 10^{18} \text{ GeV}$ the reduced Planck mass, and $G_F = 1.16 \times 10^{-5} \text{ GeV}^{-2}$ is the Fermi constant. The branching ratios into other channels are presented in Fig.1.

III. FERMI LAT LIMITS

A. Gamma-Ray Lines

Our line search is based on the measurements of the cosmic gamma-ray flux performed by the Large Area Telescope (LAT). The gamma-ray events that enter our analysis are selected from the ‘DataClean’ event class measured between 4 Aug 2008 and 17 Nov 2010. We consider energies between 1 GeV and 300 GeV, and apply the zenith angle criterion $\theta < 105^\circ$ in order to avoid contamination by the Earth’s Albedo. The expected shape of the measured gamma-ray line

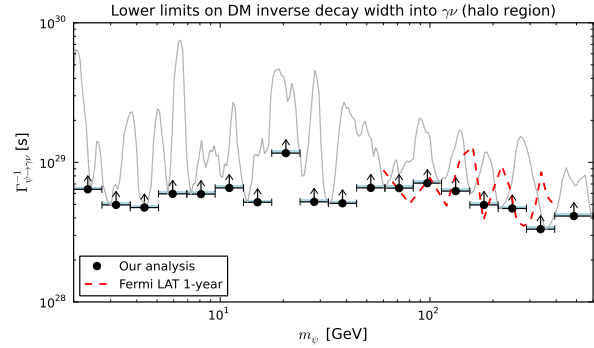


FIG. 2: Lower bounds on the dark matter inverse decay width into monochromatic photons and neutrinos as a function of the dark matter mass m_ψ , *cp.* Ref. [11]. The gray-solid line shows the 95% C.L. limits as function of the gamma-ray line energy, the black dots show the weakest limits obtained in certain adopted energy bands. The previous Fermi LAT limits from Ref. [12] are shown for comparison.

spectrum is inferred from the Fermi LAT instrument response function. In our analysis, we consider only Galactic contributions to the dark matter signal, and take the Navarro-Frenk-White (NFW) profile [12, 24] as a reference for the dark matter distribution (Einasto or isothermal profiles would lead to very similar results). All profiles are normalized to $\rho_{\text{dm}} = 0.4 \text{ GeV cm}^{-3}$ at Sun’s position. For decaying dark matter signals we choose to consider the whole sky excluding only the Galactic disk at $|b| \leq 10^\circ$ with its large foregrounds, since this large region features the best signal-to-noise ratio.

The profile likelihood method [25] is used to calculate the significance of a potential gamma-ray line contribution to the observed gamma-ray flux. The data are modeled by a simple power law plus a line signal at fixed energy E_γ . Since the power law is only locally a good approximation to the background fluxes, we use a small sliding energy window in the fitting procedure. The size of this energy window varies between $\pm 2\sigma_{\Delta E}^{68\%}$ at low gamma-ray line energies E_γ , and roughly $\frac{1}{3}E_\gamma$ to $3E_\gamma$ at high gamma-ray line energies. Lifetime upper limits at the 95% C.L. are derived by increasing the line signal and refitting the remaining parameters until the $-2\log(\text{likelihood})$ of the fit increases by 4 from its best-fit value.

No gamma-ray lines with 5σ significance were found in our analysis; the corresponding limits on dark matter decay into monochromatic photons are shown in Fig. 2.

B. Galaxy Cluster Observations

The eight galaxy clusters that we consider in this work are Fornax, Coma, A1367, A1060, AWM7, S636,

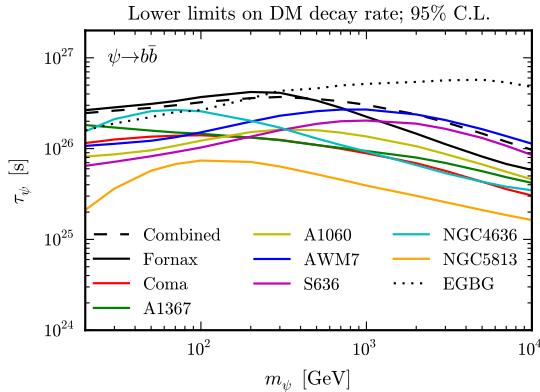


FIG. 3: Lower limits on dark matter lifetime for decay into $b\bar{b}$ final states, as function of the dark matter mass, *cp.* Ref. [13]. Solid lines show individual cluster limits, the dashed line the limits from the combined likelihood analysis. The dotted line shows for comparison the limit that can be derived from the EGBG.

NGC4636 and NGC5813. They are selected from the extended HIFLUGCS X-ray catalog [26, 27] in order to yield large signals from dark matter decay. The gamma-ray events entering our analysis are taken from the P7SOURCE.V6 event class of the Fermi LAT data measured between 4 Aug 2008 and 21 Jul 2011. From all events recorded by the Fermi LAT, we select those with energies between 400 MeV and 100 GeV and apply the zenith angle criterion $\theta < 100^\circ$ in order to avoid contamination by the Earth's Albedo. For each galaxy cluster, we consider photons events in a $10^\circ \times 10^\circ$ squared region centered on the cluster position. These events are binned into a cube of $0.1^\circ \times 0.1^\circ$ pixels with 24 logarithmic energy bins.

We assume that the smooth component of the dark matter halo follows a Navarro-Frenk-White (NFW) profile [12, 24], where the scale radius r_s and the density normalization ρ_s have to be determined from observations. We adopt the observationally obtained concentration-mass relation from Ref. [28] and use the cluster masses derived from ROSAT PSPC X-ray observations in the extended HIFLUGCS catalog [27] to calculate the signal surface densities. Gamma rays from inverse Compton scattering between the CMB and the electrons and positrons that are produced in the dark matter decay are fully taken into account.

As above, we use the profile likelihood method to fit the data with background and signal fluxes [25]. For the diffuse background fluxes we take the isotropic emission and the galactic foreground model templates currently advocated by the Fermi LAT collaboration for point source analysis (`iso_p7v6source` and `gal_2yearp7v6_v0`). On top of the diffuse templates, we add the point sources from the second Fermi LAT catalog 2FGL [29] within a radius of 12° around the cluster centers, as well as the extended dark matter signal. We account for uncertainties of the cluster

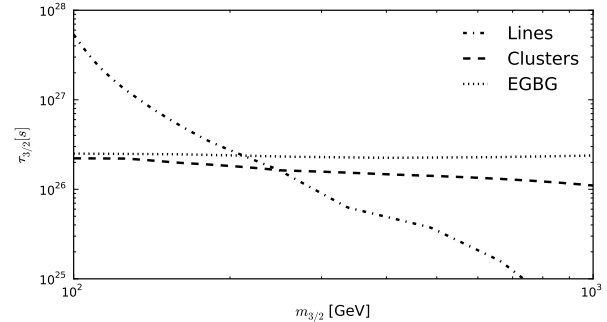


FIG. 4: Lower limits on the gravitino lifetime, *cp.* Ref. [13]. The dot-dashed line shows the gamma-ray line limits, the dashed line the limits resulting from the combined cluster analysis (using the branching ratios shown in Fig. 1), and the dotted line the EGBG limits.

masses as determined by X-ray observations as a systematic errors in our analysis. To this end, we approximate the posterior probability for the cluster masses by log-normal distributions. The resulting signal uncertainties are as large as a factor two in some cases. Finally, to combine the statistical power of the different target regions and to reduce the impact of the cluster mass uncertainties, we performed a combined likelihood analysis of all eight clusters simultaneously. In this case, the combined likelihood function is defined as the product of the likelihood functions for the individual clusters. The only parameter that is bound to be identical for all targets is the dark matter lifetime.

No significant emission from the target clusters was found. For the case of decay into $b\bar{b}$, our resulting limits are shown in Fig. 3. There, we show the limits that we obtain from the clusters individually (solid lines), as well as the limit from the combined analysis (dashed line). The dotted line shows limits derived from the extra-galactic gamma-ray background (EGBG) as measured by Fermi LAT in Ref. [30] (see Ref. [13] for details).

IV. DISCUSSION

In Fig. 4 we finally summarize the limits on the gravitino lifetime that we obtain from our gamma-ray line searches (dotdashed) and the galaxy cluster analysis (dashed). As one can see from this figure, while the search for gamma-ray lines is efficient for gravitino masses $m_{3/2} \lesssim 200$ GeV, constraints from galaxy clusters observations dominates for $m_{3/2} \gtrsim 200$ GeV. However, at high gravitino masses even stronger limits come from the measured EGBG (dotted).

A neutralino NLSP heavier than 100 GeV dominantly decays into $W^\pm \ell^\mp$ and $Z^0 \nu$. The correspond-

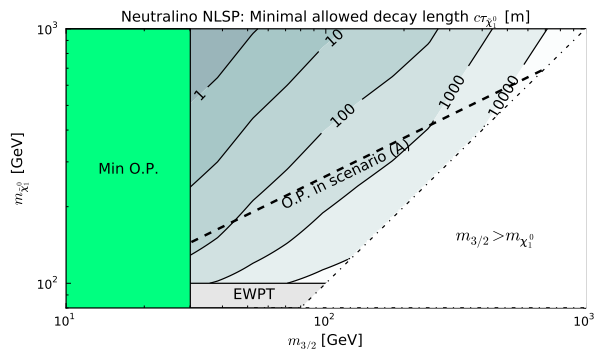


FIG. 5: Contour plot of lower bounds on the neutralino NLSP decay length, coming from both gamma-ray line and cluster constraints on the gravitino lifetime, as function of the neutralino and gravitino masses, $m_{\tilde{\chi}_1^0}$ and $m_{3/2}$ respectively, *cp.* Ref. [13]. The lower gray region is excluded by electroweak precision tests (EWPT). For thermal leptogenesis, overproduction (O.P.) of gravitinos excludes at minimum the left green region, a limit which strengthens to the black-dashed line when assuming the discussed universal boundary conditions.

ing decay width is directly proportional to ζ squared, which also enters the gravitino decay width Eq. (1). As a consequence, the two quantities can be directly related [20]. Using the above gaugino mass relation, lower bounds on the neutralino decay length $c\tau_{\tilde{\chi}_1^0}$ can be derived. Our results are summarized in Fig. 5. For the parameter space allowed by EWPT and overproduction bounds, we obtain minimal decay lengths $\mathcal{O}(100 \text{ m} - 100 \text{ km})$; decay lengths as small as $c\tau_{\tilde{\chi}_1^0} \simeq 60 \text{ m}$ are allowed for $m_{3/2} \simeq 30 \text{ GeV}$ at $m_{\tilde{\chi}_1^0} \simeq 140 \text{ GeV}$. Most interestingly, even these large decay lengths are in the range of detectability of the LHC [5], since processes like $\tilde{\chi}_1^0 \rightarrow Z^0 \nu \rightarrow \mu^+ \mu^- \nu$ with displaced vertices inside the collider would lead to essentially background free signatures [31].

Acknowledgments

CW thanks the organizers of the 2011 Fermi Symposium for an inspiring conference and the Kavli Institute for Theoretical Physics China, Beijing, for kind hospitality.

-
- [1] W. Buchmüller, L. Covi, K. Hamaguchi, A. Ibarra, and T. Yanagida, JHEP **03**, 037 (2007), hep-ph/0702184.
 - [2] F. Takayama and M. Yamaguchi, Phys. Lett. **B485**, 388 (2000), hep-ph/0005214.
 - [3] G. Bertone, W. Buchmüller, L. Covi, and A. Ibarra, JCAP **0711**, 003 (2007), 0709.2299.
 - [4] A. Ibarra and D. Tran, Phys. Rev. Lett. **100**, 061301 (2008), 0709.4593.
 - [5] K. Ishiwata, T. Ito, and T. Moroi, Phys. Lett. **B669**, 28 (2008), 0807.0975.
 - [6] K.-Y. Choi, D. E. Lopez-Fogliani, C. Munoz, and R. R. de Austri, JCAP **1003**, 028 (2010), 0906.3681.
 - [7] K.-Y. Choi, D. Restrepo, C. E. Yaguna, and O. Zapata, JCAP **1010**, 033 (2010), 1007.1728.
 - [8] J. Ke, M. Luo, L. Wang, and G. Zhu, Phys. Lett. **B698**, 44 (2011), 1101.5878.
 - [9] G. A. Gomez-Vargas et al. (2011), 1110.3305.
 - [10] W. B. Atwood et al. (Fermi LAT), Astrophys. J. **697**, 1071 (2009), 0902.1089.
 - [11] G. Vertongen and C. Weniger, JCAP **1105**, 027 (2011), 1101.2610.
 - [12] A. A. Abdo et al. (Fermi LAT), Phys. Rev. Lett. **104**, 091302 (2010), 1001.4836.
 - [13] X. Huang, G. Vertongen, and C. Weniger (2011), 1110.1529.
 - [14] M. Ackermann et al. (Fermi LAT), JCAP **1005**, 025 (2010), 1002.2239.
 - [15] L. Dugger, T. E. Jeltema, and S. Profumo, JCAP **1012**, 015 (2010), 1009.5988.
 - [16] J. R. Ellis, D. V. Nanopoulos, and S. Sarkar, Nucl. Phys. **B259**, 175 (1985).
 - [17] M. Kawasaki, K. Kohri, and T. Moroi, Phys. Rev. **D71**, 083502 (2005), astro-ph/0408426.
 - [18] M. Pospelov, Phys. Rev. Lett. **98**, 231301 (2007), hep-ph/0605215.
 - [19] M. Kawasaki, K. Kohri, T. Moroi, and A. Yotsuyanagi, Phys. Rev. **D78**, 065011 (2008), 0804.3745.
 - [20] S. Bobrovskiy, W. Buchmüller, J. Hajer, and J. Schmidt, JHEP **10**, 061 (2010), 1007.5007.
 - [21] W. Buchmüller, M. Endo, and T. Shindou, JHEP **11**, 079 (2008), 0809.4667.
 - [22] K. Nakamura et al. (Particle Data Group), J. Phys. **G37**, 075021 (2010).
 - [23] W. Buchmüller, P. Di Bari, and M. Plumacher, Ann. Phys. **315**, 305 (2005), hep-ph/0401240.
 - [24] J. F. Navarro, C. S. Frenk, and S. D. M. White, Astrophys. J. **490**, 493 (1997), astro-ph/9611107.
 - [25] W. A. Rolke, A. M. Lopez, and J. Conrad, Nucl. Instrum. Meth. **A551**, 493 (2005), physics/0403059.
 - [26] T. H. Reiprich and H. Böhringer, Astrophys. J. **567**, 716 (2002), astro-ph/0111285.
 - [27] Y. Chen, T. H. Reiprich, H. Böhringer, Y. Ikebe, and Y.-Y. Zhang, Astronomy and Astrophysics **466**, 805 (2007), astro-ph/0702482.
 - [28] D. A. Buote et al., Astrophys. J. **664**, 123 (2007), astro-ph/0610135.
 - [29] A. A. Abdo et al. (Fermi LAT) (2011), 1108.1435.
 - [30] A. A. Abdo et al. (Fermi LAT), Phys. Rev. Lett. **104**, 101101 (2010), 1002.3603.
 - [31] S. Bobrovskiy, W. Buchmüller, J. Hajer, and J. Schmidt (2011), 1107.0926.